

---

---

# Unspecific $^{18}\text{F}$ -PSMA-1007 Bone Uptake Evaluated Through PSMA-11 PET, Bone Scanning, and MRI Triple Validation in Patients with Biochemical Recurrence of Prostate Cancer

Robert Seifert<sup>1,4</sup>, Tugce Telli<sup>1,3,4</sup>, Marcel Opitz<sup>3,4,5</sup>, Francesco Barbato<sup>1,3,4</sup>, Christoph Berliner<sup>1,3,4</sup>, Michael Nader<sup>1</sup>, Lale Umutlu<sup>3-5</sup>, Martin Stuschke<sup>3,4,6</sup>, Boris Hadaschik<sup>3,4,7</sup>, Ken Herrmann<sup>1,3,4</sup>, and Wolfgang P. Fendler<sup>1,3,4</sup>

<sup>1</sup>Department of Nuclear Medicine, University Hospital Essen, Essen, Germany; <sup>2</sup>Department of Nuclear Medicine, University Hospital Münster, Münster, Germany; <sup>3</sup>German Cancer Consortium (DKTK), University Hospital Essen, Essen, Germany; <sup>4</sup>West German Cancer Center, University Hospital Essen, Essen, Germany; <sup>5</sup>Department of Diagnostic and Interventional Radiology and Neuroradiology, University Hospital Essen, Essen, Germany; <sup>6</sup>Department of Radiation Oncology, University Hospital Essen, Essen, Germany; and <sup>7</sup>Department of Urology, University Hospital Essen, Essen, Germany

J Nucl Med 2023; 64:738–743

DOI: 10.2967/jnumed.118.215434

---

$^{18}\text{F}$ -PSMA-1007 PET is used in the management of patients with prostate cancer. However, recent reports indicate a high rate of unspecific bone uptake (UBU) with  $^{18}\text{F}$ -PSMA-1007, which may lead to a false-positive diagnosis. UBU has not been evaluated thoroughly. Here, we evaluate the frequency of UBU and bone metastases separately for  $^{18}\text{F}$ -PSMA-1007 and  $^{68}\text{Ga}$ -PSMA-11 in biochemical recurrence (interindividual comparison). Additionally, we investigate UBU seen in  $^{18}\text{F}$ -PSMA-1007 through follow-up examinations (intraindividual comparison) using  $^{68}\text{Ga}$ -PSMA-11 PET, bone scintigraphy, and MRI.

**Methods:** First, all patients ( $n = 383$ ) who underwent  $^{68}\text{Ga}$ -PSMA-11 PET between January 2020 and December 2020 and all patients ( $n = 409$ ) who underwent  $^{18}\text{F}$ -PSMA-1007 PET between January 2020 and November 2021 due to biochemical recurrence were included for an interindividual comparison of bone metastases and UBU rate. In a second approach, we regarded all patients with UBU in  $^{18}\text{F}$ -PSMA-1007, characterized by focal bone uptake with an  $\text{SUV}_{\text{max}} > 4$  and prostate-specific antigen (PSA)  $\leq 5$  ng/mL, who underwent additional  $^{68}\text{Ga}$ -PSMA-11 PET ( $n = 17$ ) (interindividual comparison). Of these, 12 patients also had bone scintigraphy and whole-body MRI within a 1- to 5-wk interval. Bone uptake seen on  $^{18}\text{F}$ -PSMA-1007 but not on any of the other 4 modalities (CT, MRI [ $n = 1$ ], bone scanning, and  $^{68}\text{Ga}$ -PSMA-11 PET) was recorded as false-positive. **Results:** Patients scanned with  $^{18}\text{F}$ -PSMA-1007 PET had a significantly higher rate of UBU than those scanned with  $^{68}\text{Ga}$ -PSMA-11 (140 vs. 64;  $P < 0.001$ ); however, the rate of bone metastases was not significantly different (72 vs. 64;  $P = 0.7$ ). In the intraindividual comparison group, workup by CT, MRI, bone scanning, and  $^{68}\text{Ga}$ -PSMA-11 PET resulted in a positive predictive value for  $^{18}\text{F}$ -PSMA-1007 focal bone uptake (mean  $\text{SUV}_{\text{max}}$ ,  $6.1 \pm 2.9$ ) per patient and per lesion of 8.3% and 3.6%, respectively. **Conclusion:** In patients with PSA  $\leq 5$  ng/mL and  $\text{SUV} > 4$  at biochemical recurrence, most  $^{18}\text{F}$ -PSMA-1007 focal bone uptake is likely to be false-positive and therefore due to UBU. In the case of low clinical likelihood of metastatic disease,  $^{18}\text{F}$ -PSMA-1007 bone uptake without morphologic surrogate should be assessed carefully with regard to localization and clinical context. However, the rate of bone metastases was not higher with  $^{18}\text{F}$ -PSMA-1007 in the clinical routine, indicating that experienced reporting physicians adjust for UBU findings.

**Key Words:** prostate cancer; PET; PSMA-11; PSMA-1007

Up to 60% of prostate cancer patients develop biochemical recurrence (BCR) after initial radiotherapy or radical prostatectomy in 10 y of follow-up (1). Local salvage therapy and complete metastatic ablation of oligometastatic prostate cancer may provide a curative pathway and an alternative to initiation of palliative androgen deprivation therapy (2). Therefore, to determine location and extent of recurrent PC is of the utmost importance for directing salvage therapy.

The recent European Association of Urology Prostate Cancer guideline recommended that prostate-specific membrane antigen (PSMA) PET should be offered to BCR patients with a persistent prostate-specific antigen (PSA) level greater than 0.2 ng/mL if the results will influence subsequent treatment decisions (3). PSMA PET readers need proper training, as each PSMA ligand features distinct characteristics (4,5).

More recently,  $^{68}\text{Ga}$ -labeled PSMA ligands are increasingly replaced by  $^{18}\text{F}$ -labeled compounds offering mostly technical and logistic advantages including lower positron energy; improved spatial resolution; longer half-life; high-yield production in cyclotrons; and large batch production, thereby enabling long-distance distribution and potential cost savings (4). Moreover,  $^{18}\text{F}$ -PSMA-1007 exhibits blood clearance through the liver that leads to only minimal urinary excretion, yielding potential advantages for pelvic tumor assessment (6,7). However, unspecific bone uptake (UBU) on  $^{18}\text{F}$ -PSMA-1007 PET, reported in a considerable fraction of patients, may lead to false-positive findings as metastasis; this in turn may result in overstaging, leading to inadequate therapy (4,8,9). However, despite large observational data, UBU have not been correlated systematically by other imaging, including  $^{68}\text{Ga}$ -PSMA-11 PET/CT, MRI, and bone scanning.

Therefore, the aim of this study was 2-fold. First, we evaluated the rate of UBU and bone metastases reported in clinical reads separately for  $^{18}\text{F}$ -PSMA-1007 and  $^{68}\text{Ga}$ -PSMA-11 PET to estimate the relevance of UBUs (interindividual group). Second, we present a single-center experience with  $^{18}\text{F}$ -PSMA-1007 UBU in 17 patients, who underwent follow-up examinations to clarify the nature of the bone uptake. In those patients, we evaluated  $^{18}\text{F}$ -PSMA-1007 UBUs intraindividually with bone scanning,  $^{68}\text{Ga}$ -PSMA-11 PET, and MRI.

---

Received Aug. 13, 2022; revision accepted Nov. 17, 2022.

For correspondence or reprints, contact Robert Seifert (robert.seifert@uk-essen.de).

Published online Dec. 2, 2022.

COPYRIGHT © 2023 by the Society of Nuclear Medicine and Molecular Imaging.

## MATERIALS AND METHODS

### Patient Characteristics

Patient characteristics are shown in Table 1 and Supplemental Table 1 (supplemental materials are available at <http://jnm.snmjournals.org>). All patients were recruited at the Department of Nuclear Medicine of the University Hospital Essen. The analysis was performed retrospectively, and the need for study-specific written consent was waived (Ethics approval no. 22-10694-BO and 21-9865-BO). Briefly, 2 patient cohorts were investigated: First, the rate of UBU and bone metastases in all patients scanned with  $^{68}\text{Ga}$ -PSMA-11 in the last year before the introduction of  $^{18}\text{F}$ -PSMA-1007 was compared with the respective rates in all patients scanned with  $^{18}\text{F}$ -PSMA-1007 in the first year of its use in our Department (interindividual comparison group). Additionally, patients who received  $^{18}\text{F}$ -PSMA-1007 and underwent  $^{68}\text{Ga}$ -PSMA-11 due to  $^{18}\text{F}$ -PSMA-1007 UBU clinical workup were included (intraindividual group).

### Inclusion Criteria of the Interindividual Comparison Group

All patients who received  $^{68}\text{Ga}$ -PSMA-11 PET between January 2020 and December 2020 and all patients who received  $^{18}\text{F}$ -PSMA-1007 PET between January 2020 and November 2021 were regarded for the interindividual comparison group. Of these, 383 and 409 patients were referred to PET due to BCR or persistence and further analyzed with regard to the rate of UBU and bone metastases. For this group of patients, bone-related imaging findings were retrospectively extracted from our archives regardless of the finding's  $\text{SUV}_{\text{max}}$  and regardless of preimaging prostate-specific antigen (PSA) values in the case of histologically proven prostate

cancer and biochemical recurrence (BCR) or PSA persistence without any known metastases.

The incidence of UBU and bone metastases on  $^{18}\text{F}$ -PSMA-1007 and  $^{68}\text{Ga}$ -PSMA were compared in different preimage PSA-level groups (PSA < 1 ng/mL vs. 1–5 ng/mL vs. > 5 ng/mL).

### Inclusion Criteria of the Intraindividual Comparison Group

The  $\text{SUV}_{\text{max}}$  of UBU was reported among different studies with similar image acquisition, and the measurements ranged between 3.6 and 21.1 (4,10). Therefore, in this study, UBU was defined as focally increased  $^{18}\text{F}$ -PSMA-1007 uptake in the bone with an  $\text{SUV}_{\text{max}}$  higher than 4 and clear visualization in the maximum-intensity-projection images without CT correlate (no lytic or osteoplastic reaction). Patients with  $^{18}\text{F}$ -PSMA-1007 PET UBU were offered additional workup in the case of histologically proven prostate cancer, BCR of prostate cancer, PSA levels at the time of imaging  $\leq 5$  ng/mL, and no known distant metastases.

Patients underwent additional clinical whole-body  $^{68}\text{Ga}$ -PSMA-11 PET/MRI and bone scanning (together with SPECT/CT). Patient datasets were analyzed retrospectively.

### Imaging and Image Interpretation of the Intraindividual Comparison Group

Tracer precursors (PSMA-11 and PSMA-1007) were obtained from ABX advanced biochemical compounds (ABX GmbH).  $^{18}\text{F}$ -PSMA-1007 and  $^{68}\text{Ga}$ -PSMA-11 were synthesized on site using a kit-based approach on automated platforms with comprehensive pH, radiochemical, chemical, and radionuclide purity control tests.

After intravenous injection ( $111 \pm 20$  min) of  $^{18}\text{F}$ -PSMA-1007 ( $350.6 \pm 61.8$  MBq), PET/CT was obtained between the base of the skull and mid-thighs with the patient supine. A Biograph Vision and Biograph mCT were used for image acquisition (all: Siemens Healthineers). Full-dose CT was acquired for attenuation correction (210 mAs, 120 keV,  $512 \times 512$  matrix,  $128 \times 0.6$  mm slice thickness). PET emission data were attenuation corrected by help of the CT data and iteratively reconstructed (Vision—4 iterations; 5 subsets; voxel size,  $3.3 \times 3.3 \times 3$  mm<sup>3</sup>; Gauss filtering, 4 mm, and mCT—3 iterations; 21 subsets; voxel size;  $4.07 \times 4.07 \times 3$  mm<sup>3</sup>; Gauss filtering; 4 mm) with time-of-flight information and point-spread function correction (HD PET).

$^{68}\text{Ga}$ -PSMA-11 PET/MR ( $n = 14$ ) or PET/CT ( $n = 3$ ) was used to acquire coregistered images. The mean injected dose and mean imaging delay were  $133.3 \pm 81.2$  MBq and  $67 \pm 14$  min, respectively. PET/MRI examination was performed with an integrated 3.0-T Biograph mMR scanner (Siemens Healthineers), and simultaneous PET and 3D Dixon-volumetric interpolated breath-hold examination (VIBE) sequences for MRI-based scatter correction were performed, followed by a standardized whole-body MRI protocol. The following MR sequences of choice were acquired: high-resolution T2-weighted fast spin-echo sequences (axial, coronal, and sagittal planes), diffusion-weighted sequences (b values,  $b = 0, 500, 1,000$  s/mm<sup>2</sup>), and dynamic contrast-enhanced imaging sequences (namely, T1-weighted VIBE sequence obtained every 7 s during 5–10 min). PET emission data were iteratively reconstructed (3 iterations; 21 subsets; voxel size,  $2.09 \times 2.09 \times 2.03$  mm<sup>3</sup>, Gauss filtering, 4 mm).

Whole-body planar bone scintigraphy imaging was performed after 2.5–4 h of the administration of the median dose of 628.5 MBq (range, 584–652 MBq)  $^{99\text{m}}\text{Tc}$ -3,3-diphosphono-1,2-propanodicarboxylic acid radiopharmaceutical in a continuous mode at a rate of 15 cm/min on a  $256 \times 1,024$  acquisition matrix of anterior and posterior planes with a dual-head  $\gamma$ -camera equipped with a low-energy, high-resolution collimator (Symbia T2 or Intevo; Siemens Healthineers). In all cases of uncertain radionuclide accumulations on bone scan, SPECT/CT images were acquired (15 s/view step and shoot with  $128 \times 128$  matrix).

The time interval between the PET image acquisitions was between 1 and 5 wk. Images were interpreted using a dedicated workstation and software (SyngoVia; Siemens). All available imaging modalities were present

**TABLE 1**  
Patient Characteristics ( $n = 17$ )

Characteristic	Data
Median age (y)	71 (69.5–74)
Initial T (n)	
T1	0
T2	5 (29.5%)
T3	8 (47%)
T4	0
Unknown	4 (23.5%)
Gleason score (n)	
3 + 3	1 (5.9%)
3 + 4	2 (11.8%)
4 + 3	5 (29.4%)
4 + 4	2 (11.8%)
5 + 5	1 (5.9%)
Unknown	6 (35.3%)
Previous therapy to prostate (n)	
Radical prostatectomy	17 (100%)
Additional adjuvant/salvage radiotherapy	8 (47.1%)
Blood levels	
Median PSA (ng/mL)	0.5 (0.2–1)
Median ALP (IU/L)	70 (55–83)
Median bone-specific ALP	12.7 (11.5–17.8)

IQR = interquartile range; ALP = alkaline phosphatase.  
Data in parentheses are IQRs, unless otherwise specified.

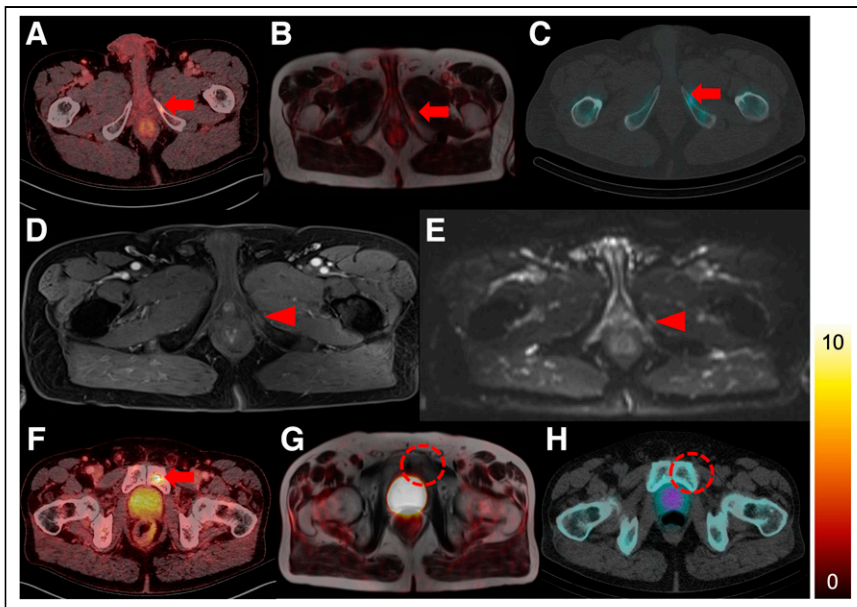


**FIGURE 1.** Exemplary cases of UBU regarded as true-positive and false-positive. Axial slices of a patient with suspected UBU on  $^{18}\text{F}$ -PSMA-1007 PET (A, arrow). Suggestive uptake was seen on  $^{68}\text{Ga}$ -PSMA-11 PET/MRI (B, arrow) and on bone scan SPECT/CT (C, arrow). Corroborating these findings, the MRI showed contrast enhancement (D, arrowhead) and diffusion restriction (E, arrowhead). Therefore, the bone uptake was rated as true-positive. A second patient is shown in F–H. Axial slices of a patient with unspecific  $^{18}\text{F}$ -PSMA-1007 uptake rated as false-positive in left inferior pubic ramus ( $\text{SUV}_{\text{max}}$ , 5.6) without any CT correlate (F, arrow) are shown. There was no suspicious finding either in  $^{68}\text{Ga}$ -PSMA-11 PET/MRI (G, dashed circle) or bone SPECT/CT (H, dashed circle). Therefore, this bone uptake was considered as false-positive.

for retrospective image reading. All PET and bone scintigraphy images were interpreted by 2 nuclear medicine physicians, and MR images were interpreted by 2 radiologists. Two nuclear medicine physicians performed semiquantitative analyses of the PET data retrospectively in consensus. For example, a focal bone uptake of  $^{18}\text{F}$ -PSMA-1007 (Fig. 1A) showing contrast enhancement (Fig. 1D), diffusion restriction (Fig. 1E), and radiotracer uptake in  $^{68}\text{Ga}$ -PSMA PET (Fig. 1B) and bone scintigraphy (Fig. 1C) was rated as bone metastasis. Conversely, a focal  $^{18}\text{F}$ -PSMA-1007 uptake of the bone without any suspicious finding on bone scan,  $^{68}\text{Ga}$ -PSMA-11, and MRI was rated as false-positive (Figs. 1F–1H).

### Statistical Analysis

SPSS Statistics (version 22; IBM Inc.) was used for statistical analyses. The compliance of variables to normal distribution was determined using the Kolmogorov–Smirnov test. Patient characteristics were presented as median (interquartile range [IQR] or range) or mean  $\pm$  SD in accordance with the data distribution. The  $\chi^2$  or Pearson goodness-of-fit tests were used to compare the differences of bone metastases and UBU in between 2 PSMA PET agents. A  $P$  value of less than 0.05 was considered statistically significant. A Sankey diagram was designed with the online Diagram Generator (Acquire Procurement Services, <http://sankey-diagram-generator.acquireprocure.com>).

## RESULTS

### Rate of Reported Bone Metastases and UBU in the Interindividual Group (Comparing $^{68}\text{Ga}$ -PSMA-11 and $^{18}\text{F}$ -PSMA-1007 Cohorts, $n = 792$ )

A total of 792 PSMA PET scans of patients with BCR were included ( $n = 409$  for  $^{18}\text{F}$ -PSMA-1007 and  $n = 383$  for  $^{68}\text{Ga}$ -PSMA-11) to evaluate the frequency of UBU and bone metastases. Among the patients who were imaged with  $^{18}\text{F}$ -PSMA-1007, 332 (81.2%), 33 (8%), 13 (3.2%), 3 (0.1%), and 115 (28.1%) patients underwent

radical prostatectomy, definitive radiotherapy, transurethral prostate resection, local ablative treatments, and adjuvant/salvage radiotherapy as previous local therapy, respectively. Among the patients who were imaged with  $^{68}\text{Ga}$ -PSMA-11, 324 (84.6%), 28 (7.3%), 7 (1.8%), 1 (0.2%), and 99 (25.8%) patients underwent radical prostatectomy, definitive radiotherapy, transurethral prostate resection, local ablative treatments, and adjuvant/salvage radiotherapy as previous local therapy, respectively. Overall, there was no statistically significant difference for the bone metastases rate when the final reports of  $^{18}\text{F}$ -PSMA-1007 and  $^{68}\text{Ga}$ -PSMA-11 were compared (72 vs. 64;  $P = 0.7$ ). Stratifying by PSA value, 229 of 397 (57.7%) patients undergoing  $^{18}\text{F}$ -PSMA-1007 and 201 of 360 (55.8%) patients undergoing  $^{68}\text{Ga}$ -PSMA-11 PET had PSA levels lower than 1 ng/mL. A fraction of the 138 of 397 (34.8%) patients undergoing  $^{18}\text{F}$ -PSMA-1007 and the 147 of 360 (40.8%) patients undergoing  $^{68}\text{Ga}$ -PSMA-11 PET had PSA levels between 1 and 5 ng/mL. Thirty of 397 (7.6%) patients undergoing  $^{18}\text{F}$ -PSMA-1007 and 12 of 360 (3.3%) patients undergoing  $^{68}\text{Ga}$ -PSMA-11 PET had  $>5$  ng/mL of PSA. There was no statistically significant difference of bone metastasis detection between  $^{18}\text{F}$ -PSMA-1007

and  $^{68}\text{Ga}$ -PSMA-11 among different PSA groups ( $P = 0.2, 0.2,$  and  $0.6$  for PSA levels groups  $< 1$  ng/mL,  $1$ – $5$  ng/mL, and  $> 5$  ng/mL, respectively) (Fig. 2).

UBU was reported at a significantly higher rate with  $^{18}\text{F}$ -PSMA-1007 than it was in the  $^{68}\text{Ga}$ -PSMA-11 group (140 [34.2%] vs. 64 [16.7%];  $P < 0.001$ ). Moreover, there was at least 1 identifiable benign bone lesion with focal PSMA uptake in 22 (5.4%) and 11 (2.9%) of the  $^{18}\text{F}$ -PSMA-1007 and  $^{68}\text{Ga}$ -PSMA-11 PET reports, respectively. There was no significant difference between the PSA-level groups and UBU rate for both agents ( $P = 0.4$  and  $0.6$ , respectively, for  $^{18}\text{F}$ -PSMA-1007 and  $^{68}\text{Ga}$ -PSMA-11).

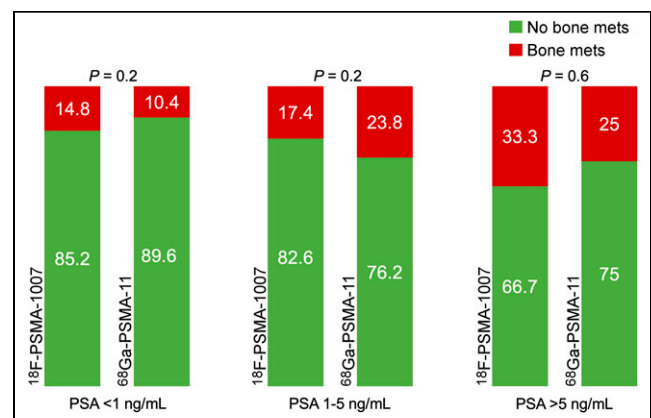


**FIGURE 2.** Frequency of bone metastases is presented separately for PSA groups and PET tracers ( $^{18}\text{F}$ -PSMA-1007 or  $^{68}\text{Ga}$ -PSMA-11). There was no statistically significant difference of bone metastasis detection between  $^{18}\text{F}$ -PSMA-1007 and  $^{68}\text{Ga}$ -PSMA-11 among 3 different PSA level groups. mets = metastasis.

### Patient Characteristics of the $^{18}\text{F}$ -PSMA-1007 and $^{68}\text{Ga}$ -PSMA-11 PET Intraindividual Comparison Cohort ( $n = 17$ )

Seventeen prostate cancer patients (mean age, 70.9 y; median duration of disease, 43.7 mo [IQR, 18.6–122.9]) underwent both  $^{68}\text{Ga}$ -PSMA-11 and  $^{18}\text{F}$ -PSMA-1007 PET due to clinical indication. The median time interval between PET scans was 22 d (IQR 8.0–29.5) days. Most patients were also evaluated with bone scanning and SPECT/CT ( $n = 14$ ) and whole-body MRI ( $n = 15$ ), and 12 patients were evaluated with all 4 modalities. All the patients had PSA recurrence after radical prostatectomy, and 8 of 17 patients also had undergone adjuvant or salvage radiation therapy. Twelve of 17 patients had a PSA level lower than 1, and 5 of 17 had PSA levels between 1 and 5 ng/mL. Further characteristics of the patients are outlined in Table 1.

Local recurrence was detected on  $^{18}\text{F}$ -PSMA-1007 in 7 (41.1%) of the patients with a median  $\text{SUV}_{\text{max}}$  of 8.1 (range, 3.48–24.6); 41.1% (7/17) of the patients were rated as pelvic lymph node-positive on  $^{18}\text{F}$ -PSMA-1007 PET. The median  $\text{SUV}_{\text{max}}$  and size of the most prominent pelvic lymph node was 10.9 (range, 3.2–37.6) and 0.5 cm (range, 0.4–1.2), respectively. Moreover, 4 patients were staged as extrapelvic lymph node-positive ( $n = 2$  inguinal and 2 retroperitoneal; median  $\text{SUV}_{\text{max}} = 5.1$  [range: 3.4–10.2]) by  $^{18}\text{F}$ -PSMA-1007 PET.

### Intraindividual Analysis of $^{18}\text{F}$ -PSMA-1007 Bone Uptake by Bone Scanning and $^{68}\text{Ga}$ -PSMA-11 PET/MRI

In  $^{18}\text{F}$ -PSMA-1007 PET, 34 suggestive bone uptake findings (in 17 patients) were seen (Supplemental Figs. 1–17 for details on patients). Evaluation of the UBUs and final decisions are summarized in Figure 3. Eleven patients (64.7%) showed unifocal, 4 patients (23.5%) showed oligofocal, and 2 patients (11.8%)

showed multifocal  $^{18}\text{F}$ -PSMA-1007 bone uptake without any correlative lesion on CT ( $n = 13$  ribs,  $n = 10$  pelvis,  $n = 4$  vertebrae,  $n = 3$  scapula,  $n = 2$  sternum,  $n = 1$  clavicle,  $n = 1$  humerus head). Distribution of the false-positive bone uptake on  $^{18}\text{F}$ -PSMA-1007 is presented in Figure 4.

The per-patient true-positive rate was 8.3%, the per-lesion ( $n = 28$ ) true-positive rate was 3.6%; the positive predictive value of bone uptake seen in  $^{18}\text{F}$ -PSMA-1007 PET was 8.3% (95% CI,  $-7\%$ –23.8%) per patient ( $n = 12$ ) and 3.6% (95% CI,  $-3.3\%$ –10.5%) per lesion ( $n = 28$ ) (only  $n = 12$  patients with all modalities, that is, MRI, bone scanning, and  $^{68}\text{Ga}$ -PSMA-11 PET, were included).

One lesion with PSMA expression ( $\text{SUV}_{\text{max}}$  6.7 and 3 on  $^{18}\text{F}$ -PSMA-1007 and  $^{68}\text{Ga}$ -PSMA-11 PET, respectively) in the left ischiopubical junction without any correlative CT lesion was regarded as true-positive because it was also positive on the bone scan and showed contrast enhancement on T1-weighted images with diffusion restriction on MRI (Fig. 1). The patient with true-positive pelvic bone metastasis had a PSA level of 0.91 ng/mL, PSA doubling time of 1 mo, 83 IU/L of alkaline phosphatase, and 21.5 ug/L of bone-specific alkaline phosphatase.

One lesion with PSMA expression ( $\text{SUV}_{\text{max}}$  6.1 and 2.3 on  $^{18}\text{F}$ -PSMA-1007 and  $^{68}\text{Ga}$ -PSMA-11 PET, respectively) without any significant CT correlation was evaluated as enchondroma on MRI (Supplemental Fig. 17). Follow-up examinations of the bone findings are summarized in Figure 3.

All other sites of  $^{18}\text{F}$ -PSMA-1007 focal bone uptake were rated as false-positive and likely UBU.

### DISCUSSION

In this article, we investigated  $^{18}\text{F}$ -PSMA-1007 PET UBU in patients with BCR by  $^{68}\text{Ga}$ -PSMA-11 PET, MRI, and bone scanning correlation. In patients with correlative imaging, the positive predictive value of  $^{18}\text{F}$ -PSMA-1007 PET for bone metastases was very low. We present a systematic confirmation of  $^{18}\text{F}$ -PSMA-1007 PET UBU. However, the higher rate for  $^{18}\text{F}$ -PSMA-1007 than for  $^{68}\text{Ga}$ -PSMA-11 PET did not translate into more frequent diagnosis of bone metastases if images were read by experienced readers.

PSMA PET has become the reference standard examination of the staging and restaging of patients with prostate cancer (11,12). It was shown previously that PSMA PET is superior to CT and bone scanning in primary staging of patients with high-risk prostate cancer (12). PSMA-11 was assessed in most prospective trials on PSMA-directed imaging, which led to recent Food and Drug Administration approval. Several other PSMA ligands have been studied. For example,  $^{18}\text{F}$ -DCF-Pyl showed high diagnostic accuracy and was also approved by the Food and Drug Administration (13). Head-to-head comparison of  $^{18}\text{F}$ -DCF-Pyl and  $^{18}\text{F}$ -PSMA-1007 revealed near equal tumor detection in a small group of patients with newly diagnosed prostate cancer (14). In France, the ligand  $^{18}\text{F}$ -PSMA-1007 is available through expanded access.

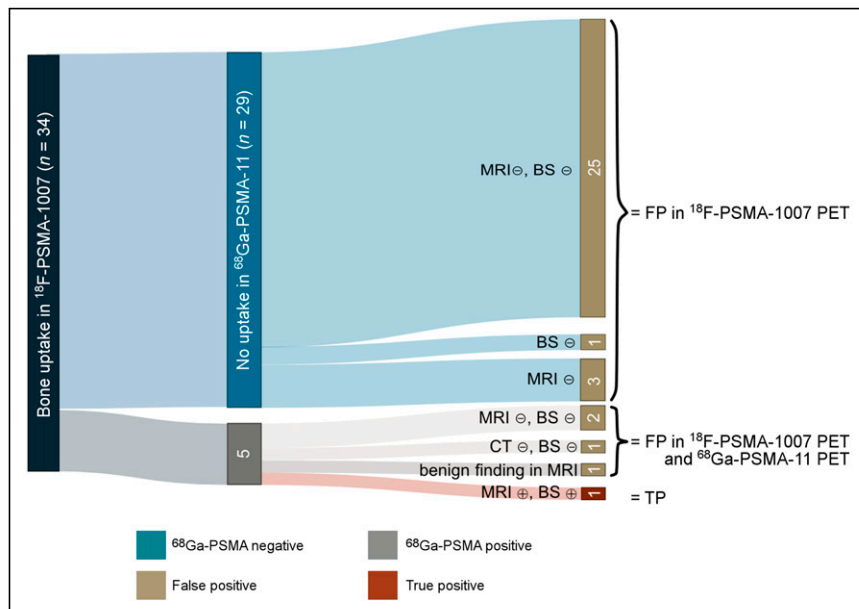


**FIGURE 3.** Sankey Diagram summarizing the evaluation of UBUs seen in  $^{18}\text{F}$ -PSMA-1007 PET. BS = bone scan; FP = false-positive; TP = true-positive; PSMA = prostate-specific membrane antigen; ⊖ = no suspicious finding; ⊕ = suspicious finding. A total number of 34 UBUs were detected on  $^{18}\text{F}$ -PSMA-1007 PET. One lesion was regarded as true-positive (bone metastasis) and 1 lesion was rated as benign because of characteristic MRI findings. Thirty-three UBU were rated as false-positive on  $^{18}\text{F}$ -PSMA-1007 PET and 4 instances of false-positive bone uptake were seen on  $^{68}\text{Ga}$ -PSMA-11 PET (triple validation was only available in a subcohort).



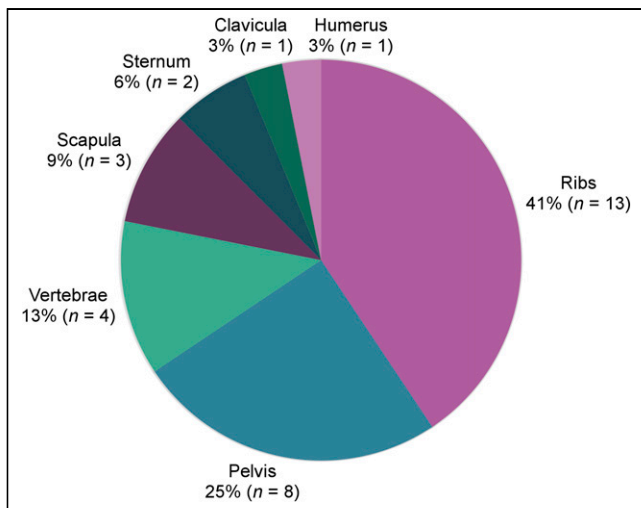


**FIGURE 4.** Anatomic distribution of UBU seen on  $^{18}\text{F}$ -PSMA-1007 PET. Thirty-two instances of bone uptake were seen on  $^{18}\text{F}$ -PSMA-1007 PET (in multiple regions) and 4 instances of bone uptake were seen on  $^{68}\text{Ga}$ -PSMA-11 (all located in ribs). Most common UBU localizations for  $^{18}\text{F}$ -PSMA-1007 were ribs and pelvis.

PSMA ligands show comparable tumor uptake and distribution, but also have distinctive biodistribution features (5).  $^{18}\text{F}$ -PSMA-1007 has a liver-dominant excretion, which offers advantages for the assessment of local prostate cancer infiltration (6). Because of lesser ligand accumulation in the bladder, the differentiation between true tracer uptake and urinary background activity is often easier, which facilitates the detection of local recurrence.

The rise of  $^{18}\text{F}$ -PSMA-1007 is mainly caused by the ease of cyclotron-based  $^{18}\text{F}$ -fluorine production, which enables the syntheses of larger quantities of PSMA ligands compared with  $^{68}\text{Ga}$  generators (4). Additionally,  $^{18}\text{F}$ -fluorine offers a longer half-life than  $^{68}\text{Ga}$ , enabling an optimized patient management (4). Moreover, the lower positron energy of  $^{18}\text{F}$  enables a higher spatial resolution and higher signal-to-background ratio than  $^{68}\text{Ga}$  (4).

Despite these benefits of  $^{18}\text{F}$ -PSMA-1007, it has been reported that the rate of UBU is notably higher than that of  $^{68}\text{Ga}$ -PSMA-11 (8,15). In our study, 33 UBUs have been reported for  $^{18}\text{F}$ -PSMA-1007 PET and 4 for  $^{68}\text{Ga}$ -PSMA-11 (triple validation was available only in a subcohort). This makes the clear delineation of bone metastases challenging in patient cohorts in which bone metastases have a low prevalence, such as in men with biochemically recurrent prostate cancer at low PSA level. The false-positive assessment of bone uptake may potentially lead to inadequate treatment when anticipating that  $^{18}\text{F}$ -PSMA-1007 has the same high specificity of other PSMA ligands.

UBU has also been reported in other PSMA-targeting tracers. For example, preliminary reports indicate that rhPSMA-7 also shows UBU (16). The cause of UBU is not yet known. Unconjugated fluorine, activated bone marrow granulocytes (15), and PSMA expression in nonprostate cancer tissue have been discussed previously (17,18).

Interestingly, UBUs of  $^{18}\text{F}$ -PSMA-1007 show a distinct distribution pattern. Especially, uptake in the ribs and pelvis can be observed, yet the explanation for this is unknown. Despite a higher UBU rate for  $^{18}\text{F}$ -PSMA-1007, the rate of bone metastases was not different in the cohorts of patients imaged with  $^{18}\text{F}$ -PSMA-1007

versus  $^{68}\text{Ga}$ -PSMA-11 in patients with BCR. For this, all patients scanned in the year before transition to  $^{18}\text{F}$ -PSMA-1007 were compared with all patients scanned in the year after the tracer switch. This observation indicates that experienced nuclear medicine physicians can detect the UBU pattern and identify the lesions as un-specific. The distinctive pattern of UBU at the above-described locations may contribute to this observation. Current knowledge on UBU for  $^{18}\text{F}$ -PSMA-1007 and radioligands with similar bone pattern should be summarized in a comprehensive reader training before local implementation of these tracers.

This study comes with limitations. First, the comparisons of patient cohorts before and after the change of PSMA tracers (from  $^{68}\text{Ga}$ -PSMA-11 to  $^{18}\text{F}$ -PSMA-1007) were analyzed retrospectively. Therefore, the analysis might be prone to selection bias and missing information. In the subgroup of patients undergoing MRI, bone scanning, and  $^{68}\text{Ga}$ -PSMA-11 as well as  $^{18}\text{F}$ -PSMA-1007 PET, the additional PSMA PET and bone scintigraphy were performed only when clinically indicated and after patient approval and the data collection was done retrospectively. Therefore, our cohort with 4 imaging assessments was relatively small, and the results may not be transferable to larger cohorts. Finally, histopathologic confirmation and follow-up imaging were not acquired for this study.

## CONCLUSION

In patients with BCR of prostate cancer and  $\text{PSA} \leq 5 \text{ ng/mL}$ , focal bone uptake on  $^{18}\text{F}$ -PSMA-1007 PET ( $\text{SUV} > 4$ ) was most often false-positive/UBU when compared with  $^{68}\text{Ga}$ -PSMA-11 PET, MRI, and bone scanning.  $^{18}\text{F}$ -PSMA-1007 false-positive/UBU findings were most commonly located in the ribs and pelvis. Bone uptake in  $^{18}\text{F}$ -PSMA-1007 and  $^{18}\text{F}$  radioligands with similar bone pattern should therefore be evaluated carefully with regards to the location and clinical context. Most likely due to reader experience, the rate of bone metastases was not higher when clinical cohorts of patients with BCR imaged with  $^{68}\text{Ga}$ -PSMA-11 and  $^{18}\text{F}$ -PSMA-1007 were compared. To prevent false bone upstaging and consequently incorrect therapy management of the patients,  $^{18}\text{F}$ -PSMA-1007 PET should be performed by experienced physicians with knowledge of UBU distribution pattern and characteristics

## DISCLOSURE

Wolfgang P. Fendler reports fees from SOFIE Bioscience (research funding), Janssen (consultant, speakers bureau), Calyx (consultant), Bayer (consultant, speakers bureau, research funding), Parexel (image review), and AAA (speakers bureau) outside of the submitted work. Boris Hadaschik has had advisory roles for ABX, AAA/Novartis, Astellas, AstraZeneca, Bayer, Bristol Myers Squibb, Janssen R&D, Lightpoint Medical, Inc., and Pfizer; has received research funding from Astellas, Bristol Myers Squibb, AAA/Novartis, German Research Foundation, Janssen R&D, and Pfizer; and has received compensation for travel from Astellas, AstraZeneca, Bayer and Janssen R&D. Robert Seifert has received research funding from the Else Kröner-Fresenius-Stiftung and Boehringer Ingelheim Fonds. No other potential conflict of interest relevant to this article was reported.

## ACKNOWLEDGMENT

We thank Andrei Iagaru for his support in revising the article.

## KEY POINTS

**QUESTION:** How clinically relevant is the previously reported occurrence of UBU on <sup>18</sup>F-PSMA-1007 PET in prostate cancer?

**PERTINENT FINDINGS:** Bone uptake seen on <sup>18</sup>F-PSMA-1007 PET in patients with BCR, PSA ≤ 5 ng/mL, and SUV > 4 is likely false-positive. Common locations for false positive findings were ribs and pelvis. However, in the clinical routine, the rate of reported bone metastases of patients imaged with <sup>18</sup>F-PSMA-1007 or <sup>68</sup>Ga-PSMA-11 is comparable, indicating that reporting physicians adapt to the tracer characteristics.

**IMPLICATIONS FOR PATIENT CARE:** When metastatic disease is suspected in biochemical recurrent prostate cancer, osseous <sup>18</sup>F-PSMA-1007 uptake without morphologic correlate has to be carefully assessed.

## REFERENCES

1. Mullins JK, Feng Z, Trock BJ, Epstein JI, Walsh PC, Loeb S. The impact of anatomical radical retropubic prostatectomy on cancer control: the 30-year anniversary. *J Urol*. 2012;188:2219–2224.
2. Phillips R, Shi WY, Deek M, et al. Outcomes of observation vs stereotactic ablative radiation for oligometastatic prostate cancer: The ORIOLE phase 2 randomized clinical trial. *JAMA Oncol*. 2020;6:650–659.
3. Cornford P, van den Bergh RCN, Briers E, et al. EAU-EANM-ESTRO-ESUR-SIOG guidelines on prostate cancer: part ii—2020 update: treatment of relapsing and metastatic prostate cancer. *Eur Urol*. 2021;79:263–282.
4. Rauscher I, Krönke M, König M, et al. Matched-pair comparison of <sup>68</sup>Ga-PSMA-11 PET/CT and <sup>18</sup>F-PSMA-1007 PET/CT: frequency of pitfalls and detection efficacy in biochemical recurrence after radical prostatectomy. *J Nucl Med*. 2020;61:51–57.
5. Eiber M, Herrmann K, Calais J, et al. Prostate cancer molecular imaging standardized evaluation (PROMISE): proposed miTNM classification for the interpretation of PSMA-ligand PET/CT. *J Nucl Med*. 2018;59:469–478.
6. Dietlein F, Kobe C, Hohberg M, et al. Intraindividual comparison of <sup>18</sup>F-PSMA-1007 with renally excreted PSMA ligands for PSMA PET imaging in patients with relapsed prostate cancer. *J Nucl Med*. 2020;61:729–734.
7. Seifert R, Schafigh D, Bogemann M, Weckesser M, Rahbar K. Detection of local relapse of prostate cancer with <sup>18</sup>F-PSMA-1007. *Clin Nucl Med*. 2019;44:e394–e395.
8. Armfield EG, Thomas PA, Roberts MJ, et al. Clinical insignificance of [<sup>18</sup>F]PSMA-1007 avid non-specific bone lesions: a retrospective evaluation. *Eur J Nucl Med Mol Imaging*. 2021;48:4495–4507.
9. Pattison DA, Debowski M, Gulhane B, et al. Prospective intra-individual blinded comparison of [<sup>18</sup>F]PSMA-1007 and [<sup>68</sup>Ga]Ga-PSMA-11 PET/CT imaging in patients with confirmed prostate cancer. *Eur J Nucl Med Mol Imaging*. 2022;49:763–776.
10. Vollnberg B, Alberts I, Genitsch V, Rominger A, Afshar-Oromieh A. Assessment of malignancy and PSMA expression of uncertain bone foci in [<sup>18</sup>F]PSMA-1007 PET/CT for prostate cancer—a single-centre experience of PET-guided biopsies. *Eur J Nucl Med Mol Imaging*. 2022;49:3910–3916.
11. Fendler WP, Calais J, Eiber M, et al. Assessment of <sup>68</sup>Ga-PSMA-11 PET accuracy in localizing recurrent prostate cancer: a prospective single-arm clinical trial. *JAMA Oncol*. 2019;5:856–863.
12. Hofman MS, Lawrentschuk N, Francis RJ, et al. Prostate-specific membrane antigen PET-CT in patients with high-risk prostate cancer before curative-intent surgery or radiotherapy (proPSMA): a prospective, randomised, multicentre study. *Lancet*. 2020;395:1208–1216.
13. Morris MJ, Rowe SP, Gorin MA, et al. Diagnostic performance of <sup>18</sup>F-DCFPyL-PET/CT in men with biochemically recurrent prostate cancer: results from the CONDOR phase III, multicenter study. *Clin Cancer Res*. 2021;27:3674–3682.
14. Giesel FL, Will L, Lawal I, et al. Intraindividual comparison of <sup>18</sup>F-PSMA-1007 and <sup>18</sup>F-DCFPyL PET/CT in the prospective evaluation of patients with newly diagnosed prostate carcinoma: a pilot study. *J Nucl Med*. 2018;59:1076–1080.
15. Grünig H, Maurer A, Thali Y, et al. Focal unspecific bone uptake on [<sup>18</sup>F]PSMA-1007 PET: a multicenter retrospective evaluation of the distribution, frequency, and quantitative parameters of a potential pitfall in prostate cancer imaging. *Eur J Nucl Med Mol Imaging*. 2021;48:4483–4494.
16. Eiber M, Kroenke M, Wurzer A, et al. <sup>18</sup>F-rhPSMA-7 PET for the detection of biochemical recurrence of prostate cancer after radical prostatectomy. *J Nucl Med*. 2020;61:696–701.
17. Silver DA, Pellicer I, Fair WR, Heston WD, Cordon-Cardo C. Prostate-specific membrane antigen expression in normal and malignant human tissues. *Clin Cancer Res*. 1997;3:81–85.
18. Backhaus P, Noto B, Avramovic N, et al. Targeting PSMA by radioligands in non-prostate disease—current status and future perspectives. *Eur J Nucl Med Mol Imaging*. 2018;45:860–877.